Low-energy surface phonons of decagonal and icosahedral quasicrystals by inelastic He-atom scattering

H. R. Sharma,[1] K. J. Franke,[1] W. Theis,[1,*] P. Gille,[2] Ph. Ebert,[3] and K. H. Rieder[1]
[1]*Institut für Experimentalphysik der Freie Universität Berlin, 14195 Berlin, Germany*
[2]*Sektion Kristallographie, Department für Geo- und Umweltwissenschaften, Ludwig-Maximilians-Universität München, 80333 München, Germany*
[3]*Institut für Festkörperforschung, Forschungszentrum Jülich GmbH, 52425 Jülich, Germany*
(Received 17 April 2003; published 19 August 2003)

Low-energy surface phonons (Rayleigh mode) on quasicrystals were investigated by inelastic He-atom scattering. The tenfold surface of decagonal $Al_{71.8}Ni_{14.8}Co_{13.4}$ and the fivefold surface of icosahedral $Al_{70.5}Pd_{21}Mn_{8.5}$ are found to possess well-defined Rayleigh modes with isotropic sound velocities of about 3840 m/s and 3470 m/s, respectively. The observed sound velocities are in good agreement with calculations based on the respective bulk data. The experimental phonon dispersions exhibit quasi-Brillouin-zone centers located at strong Bragg peaks.

DOI: 10.1103/PhysRevB.68.054205 PACS number(s): 61.44.Br, 68.35.Ja, 68.49.Bc, 63.22.+m

I. INTRODUCTION

Since their discovery in 1984,[1] quasicrystals have become an interesting topic for theoretical and experimental investigations. Perfect long-range order in combination with the lack of translational symmetry is the most striking feature of quasicrystalline alloys. Aside from their intriguing structure and their outstanding bulk properties, quasicrystals exhibit many interesting surface characteristics. While significant progress has been made in various domains of surface science of quasicrystals such as structure and physical properties,[2,3] experimental knowledge regarding the nature of low-energy surface vibrations had still been lacking.

Theoretical[4–8] and experimental investigations of bulk phonons[9–17] show that quasicrystals, as periodic crystals, exhibit well-defined acoustic modes in the continuum limit. Phonons in periodic crystals have a well-defined energy and wave vector due to the lattice periodicity and phonon modes can be fully characterized by a wave vector confined to the first Brillouin zone and a band index.[18] Due to the lack of periodicity a Brillouin zone cannot be properly defined in quasicrystals. However, the positions of strong Bragg peaks act as quasi-Brillouin-zone (QBZ) centers.[19,20] The QBZ boundaries are packed hierarchically around the zone centers. The dispersion curves originate from the QBZ centers, follow a linear relation up to a certain wave vector, and finally become dispersionless at the QBZ boundaries. Experimental studies reveal that bulk phonon peak widths are limited by the instrumental resolution up to a certain wave vector and increase rapidly for larger wave vectors.[9,16]

This paper reports the results of low-energy surface phonons (Rayleigh mode) of decagonal and icosahedral quasicrystals investigated by inelastic He-atom scattering. The Rayleigh waves propagate along the surface with the polarization vector (direction of displacement of atoms) lying in the sagittal plane (the plane defined by the surface normal and propagation direction of the wave). In the continuum limit the displacement of atoms decays exponentially with distance from the surface into the bulk.[21] Two different quasicrystals, namely, decagonal (*d*) $Al_{71.8}Ni_{14.8}Co_{13.4}$ and icosahedral (*i*) $Al_{70.5}Pd_{21}Mn_{8.5}$ were studied. These two quasicrystals are the most common systems used for surface studies due to the availability of large single grain samples. The decagonal quasicrystal belongs to the class of 2D quasicrystals with quasicrystalline planes stacked periodically. In contrast to two-dimensional (2D) quasicrystals, the icosahedral quasicrystal has quasicrystalline order in all three dimensions. The high symmetry surfaces of these quasicrystals (the tenfold *d*-Al-Ni-Co and fivefold *i*-Al-Pd-Mn) are found to possess well-defined Rayleigh modes.

II. EXPERIMENT

Single grain *d*-$Al_{71.8}Ni_{14.8}$ $Co_{13.4}$ and *i*-$Al_{70.5}Pd_{21}Mn_{8.5}$ quasicrystals were grown by the Czochralski method.[24,23,22] The *i*-Al-Pd-Mn was annealed for three months at 820 °C, Refs. 25 and 26. The samples were cut and polished perpendicular to the tenfold and fivefold axes, respectively, before surface treatment in the He-atom scattering chamber (base pressure 2×10^{-10} mbar). The surfaces were prepared by sputtering (Ne^+, 1–5 keV) and annealing at 650 °C and 850 °C, respectively. The quality of the surface was examined after each sputter-annealing cycle by monitoring the He specular (reflected) intensity. The cleaning processes were repeated until an optimum specular intensity was obtained.

The surface phonons were measured by inelastic He-atom scattering in a time-of-flight (TOF) setup. Details of the TOF setup are discussed in Ref. 27. The key idea is that the He-atom beam is scattered from the surface and the time of flight of inelastically scattered He atoms is measured. The time of flight along with other experimental parameters such as total scattering angle (90°), beam energy, and angle of incidence θ_i determine the energy and parallel momentum transfer on the basis of energy and momentum conservation.[28]

The TOF spectra were recorded at an elevated sample temperature. This has two important advantages. First, due to the low intensity of inelastically scattered He atoms, the measurement time of each TOF spectrum has to be fairly long to observe pronounced phonon peaks (each of the spectra presented here was recorded for 3 h). However, at room temperature the surface contaminates within a few hours due

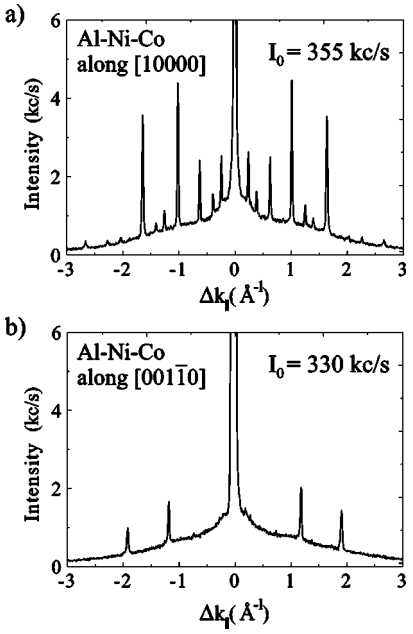

FIG. 1. He diffraction from the tenfold *d*-Al-Ni-Co surface recorded along [10000] (a) and [00$\bar{1}$0] (b) azimuths at a beam energy of 22 meV.

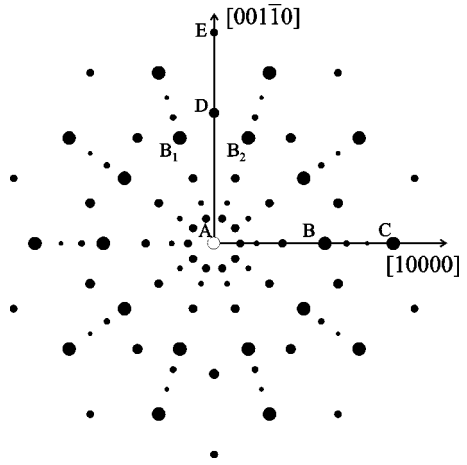

FIG. 2. He diffraction pattern from the tenfold *d*-Al-Ni-Co surface assembled from the line scans in Fig. 1 by tenfold symmetrization. The area of solid circles is proportional to the He scattering intensity (the specular intensity is not drawn to scale). The diffraction spot *B* reflects the peak at $\Delta k_{||} = 1.02$ Å^{-1} in Fig. 1(a).

to adsorption of residual gases present in the ultrahigh vacuum chamber. Keeping the sample at elevated temperature preserves the surface from getting contaminated too quickly. Second, at higher temperature the population of phonons is increased. This results in a larger probability of phonon creation and annihilation in the scattering process, increasing the intensity of the phonon peaks. On the other hand, as the temperature is increased, multiphonon events begin to dominate over single phonon events. The optimum temperature was found to be around 200 °C and all TOF spectra presented here were recorded at this temperature.

III. RESULTS AND DISCUSSION

A. The tenfold *d*-Al-Ni-Co surface

The tenfold *d*-Al-Ni-Co surface includes two inequivalent sets of high symmetry directions appearing alternately at 18°, which can be represented by [10000] and [00$\bar{1}$0].[29] Helium diffraction spectra along these two directions are shown in Fig. 1. The small width and the high overall intensity of the diffraction peaks reveals a high structural quality of the surface. The observed peak positions are consistent with those of a bulk terminated surface.

To gain an impression of the structure of the reciprocal lattice of the surface, the He peak intensities from the line scans (Fig. 1) are compiled in a two-dimensional intensity distribution in Fig. 2. Low-energy electron diffraction (LEED) reveal that diffraction spots along non-twofold directions are significantly weaker. Along the [10000] azimuth, the peaks at 1.02 Å^{-1} (*B*) and 1.65 Å^{-1} (*C*) are strongest, while the strongest peaks along [00$\bar{1}$0] are at 1.2 Å^{-1} (*D*) and 1.94 Å^{-1} (*E*). The relevant QBZ centers for measurements along the twofold azimuths are thus expected at these positions and the QBZ boundaries at the midpoint of *AB*,*BC*,*AD*, and *DE*.

A representative TOF spectrum recorded at $\theta_i = 42.7°$ along [00$\bar{1}$0] is shown in Fig. 3. It consists of a dominant elastic peak, two phonon creation peaks, and a broad background. The elastic peak is due to diffuse scattering from

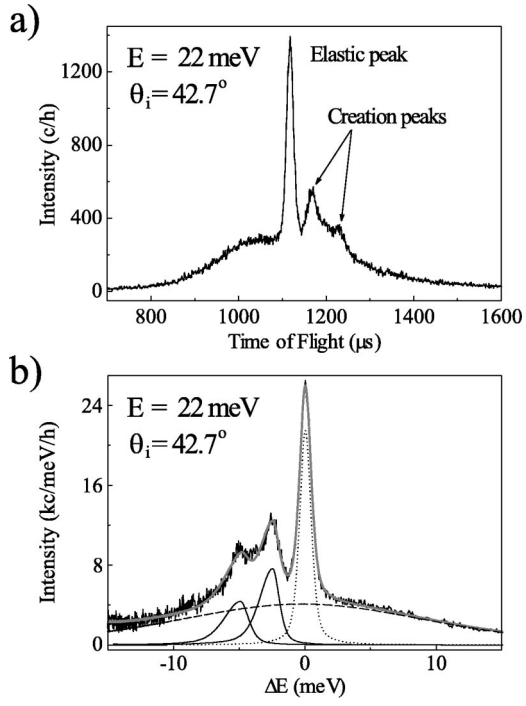

FIG. 3. (a) A representative TOF spectrum from the tenfold surface of *d*-Al-Ni-Co recorded at $\theta_i = 42.7°$ in the [00$\bar{1}$0] azimuth. The sample temperature was around 200 °C. (b) Same spectrum plotted versus energy transfer. (Solid gray curve, total fit; solid curve, phonon peak; dotted curve, elastic peak; and dashed curve, background.)

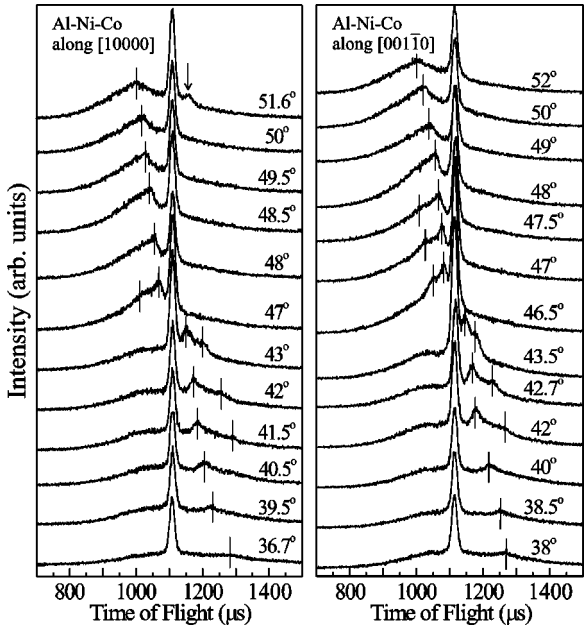

FIG. 4. Sets of TOF spectra from the tenfold *d*-Al-Ni-Co surface along the [10000] and $[00\bar{1}\bar{1}0]$ azimuths. Beam energy was 22 meV, sample temperature around 200 °C. The angles of incidence are shown above the spectra. The positions of single phonon peaks are marked by vertical lines. The peak indicated by an arrow is a decepton.

defects. The background intensity arises from contributions of multiple surface phonons and the continuum of surface projected bulk bands. Creation peaks appear at longer flight time than the elastic peak due to the loss of kinetic energy of the He atom during scattering. The intensity as a function of energy transfer is shown in Fig. 3(b). To determine the position and width of the phonon peaks the data were fitted by empirical line shapes (single phonon, sum of asymmetric Gaussian and Lorentzian; diffuse elastic peak and background, sum of Gaussian and Lorentzian). The total fit as well as the individual elastic, inelastic, and background components are shown in the figure. The widths of the creation peaks are dominated by the instrumental broadening. The presence of well-defined inelastic peaks demonstrates that the inelastic processes have a significant single phonon contribution.

In order to obtain the experimental surface phonon dispersion, TOF spectra were recorded as a function of incident angle θ_i for several He beam energies from 10 meV to 33 meV along the two high symmetry [10000] and $[00\bar{1}\bar{1}0]$ directions. Selected TOF spectra at 22 meV beam energy are shown in Fig. 4. The positions of single phonon peaks are marked by vertical lines. An additional peak indicated by an arrow in the topmost spectrum of Fig. 4, left, is not due to single phonon scattering. The angle $\theta_i = 51.6°$ at which the TOF spectrum is measured is very close to a diffraction peak at 52.6° ($\Delta k_{\parallel} = 1.02$ Å^{-1}). The diffraction peak contains a broad, low-intensity tail derived from the velocity distribution of the incident He beam which causes the appearance of the additional elastic peak, a so-called decepton.[28]

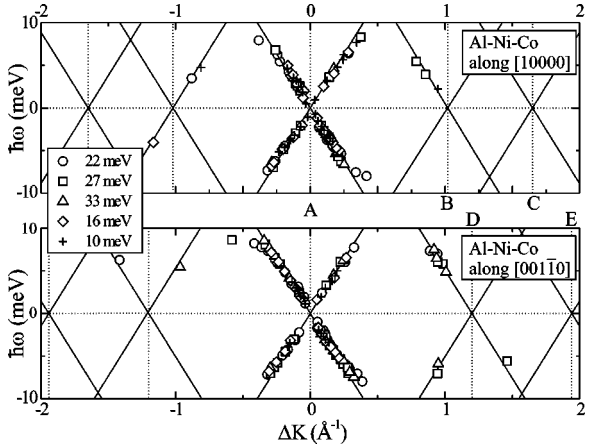

FIG. 5. The phonon dispersion relation of the tenfold *d*-Al-Ni-Co surface along [10000] (top) and $[00\bar{1}\bar{1}0]$ azimuths (bottom). Different symbols represent the data obtained for different beam energies. The solid lines represent the linear dispersion expected from elastic moduli (Ref. 30) ($v_R = 3840$ m/s).

The energy and momentum transfer of the single phonon creation and annhilation peaks yield the individual points of the experimental dispersion shown in Fig. 5. The data are plotted in an extended zone, since for quasicrystals that lack periodicity, the reduced BZ representation is not well defined. However, a folding into the first quadrant of (ω,k) space is still possible and illustrated in Fig. 6. The experimental dispersion reveals an acoustic branch (Rayleigh mode) originating from $\Delta K = 0$ and strong reciprocal lattice points (B and D).

The expected initial slope for long wavelengths can be calculated from the elastic moduli and density which were reported by Chernikov *et al.*[30] For the tenfold surface, the Rayleigh velocity v_R is given by the smallest root of $c_{33}c_{55}\rho^2 v^4(c_{11} - \rho v^2) = (c_{55} - \rho v^2)[c_{33}(c_{11} - \rho v^2) - c_{13}^2]^2$,

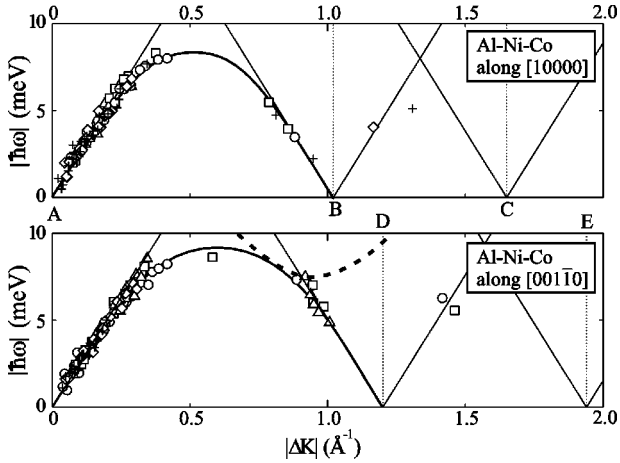

FIG. 6. The dispersion curves of the tenfold *d*-Al-Ni-Co surface along [10000] (top) and $[00\bar{1}\bar{1}0]$ azimuths (bottom) folded into the first quadrant of (ω,k) space. Symbols as in Fig. 5. The thick solid lines serve as guides to the eye. The dashed line represents the linear dispersion originating from QBZ centers B_1 and B_2 on the neighboring [10000] equivalent azimuths (see Fig. 2).

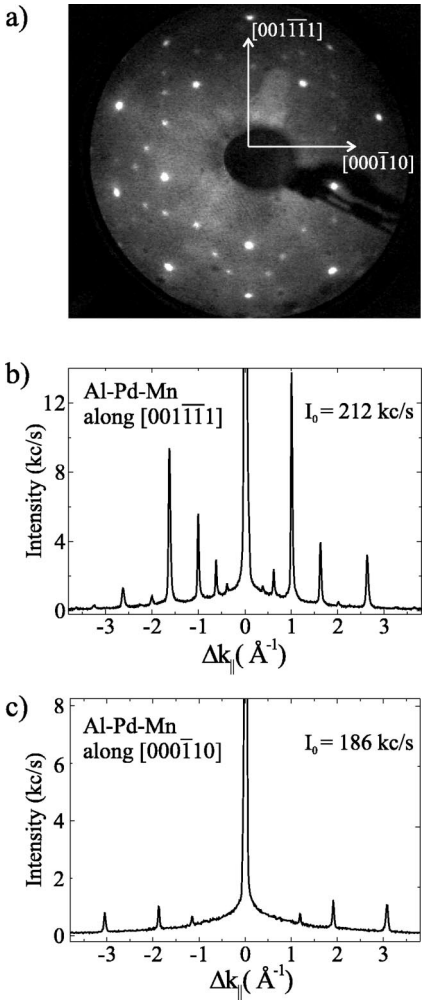

FIG. 7. Diffraction from the fivefold *i*-Al-Pd-Mn(100000) surface. LEED at 88.4 eV electron energy (a), He diffraction along the $[001\bar{1}\bar{1}1]$ (b), and $[000\bar{1}10]$ (c) directions at 22 meV beam energy.

as derived in Ref. 31. This yields $v_R = 3840$ m/s, which is represented by solid lines in Figs. 5 and 6 and in excellent agreement with our experimental dispersion.

The dispersion follows the initial slope up to around 0.30 Å^{-1} (energy 7.5 meV). Beyond this value, a tendency of the dispersion to level off towards the QBZ boundaries can be observed (Fig. 6). However, a reliable determination of the phonon energy at the QBZ boundaries is not possible since the single phonon peaks in the TOF spectra vanish in the Gaussian background as they approach the QBZ boundary.

So far only QBZ centers which lie in the azimuth for which the dispersion is being measured have been discussed. However, all reciprocal lattice vectors of the surface constitute QBZ centers which are expected to exhibit modes with an initial linear dispersion. In periodic systems (with one atom per unit cell for simplicity) all of these reflect just one single phonon mode and the dispersion can be represented in the reduced zone scheme. In quasicrystals, however, this is not the case and the detailed distribution of QBZ centers becomes important.

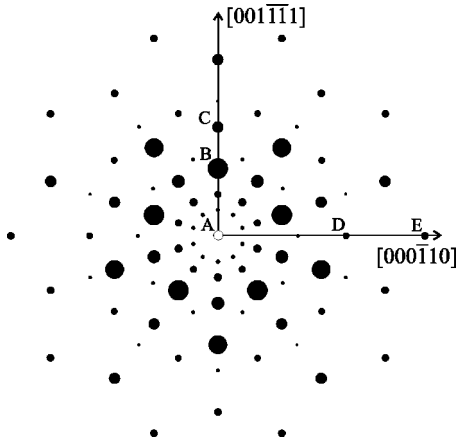

FIG. 8. He diffraction of the fivefold *i*-Al-Pd-Mn(100000) surface represented by solid circles. The area of circles is proportional to the intensity (the specular intensity is not to scale). The diffraction spot *B* reflects the peak at $\Delta k_{\|} = 0.99$ Å^{-1} in Fig. 7(b).

Consider the dispersion along $[00\bar{1}\bar{1}0]$. As can be seen in Fig. 2, two strong diffraction peaks B_1 and B_2 are located close to the $[00\bar{1}\bar{1}0]$ axis. An isotropic linear dispersion with the Rayleigh velocity originating from these points cuts the $[00\bar{1}\bar{1}0]$ axis resulting in a parabolic dispersion (dashed line in Fig. 6). In the minimum, its **k** vector difference to the Bragg points B_1 and B_2 is exactly perpendicular to the experimental momentum transfer. Therefore, the He-atom cross section is expected to be extremely small. This also holds to a lesser degree for the vicinity of the minimum and the rest of the dashed line. Thus, it is not surprising that no related phonon peaks are observed in He-atom scattering. All other off-azimuth Bragg peaks are even weaker or further from the relevant azimuth and do not need to be considered.

For the bulk phonons it was found in neutron scattering experiments[16] that the phonon peak widths increase rapidly beyond the linear regime of the dispersion which extended up to approximately 0.30 Å^{-1}. In our data the phonon peak height monotonically decreases with increasing wave vector (see Fig. 4, wave vector increases as θ_i moves away from 45°). Such a decrease is expected in He-atom scattering due to the strong attenuation of the cross section with increasing wave vector and energy transfer. For small wave vectors, the phonon peaks have sufficiently high intensity to determine the width with a relatively small error. In contrast, at larger wave vectors the intensity of the peaks is very low compared to the Gaussian background and the peak shape cannot be determined exactly. Because of these ill-defined phonon peaks for larger wave vectors, it is not possible to determine whether the surface phonon peaks exhibit a strong increase of intrinsic width beyond a specific momentum as observed for bulk phonons.

B. The fivefold *i*-Al-Pd-Mn surface

In addition to the tenfold surface of *d*-Al-Ni-Co, we studied the fivefold *i*-Al-Pd-Mn(100000) surface. While the rotational symmetry of this surface is smaller, the icosahedral symmetry results in an elastically isotropic[32] material in con-

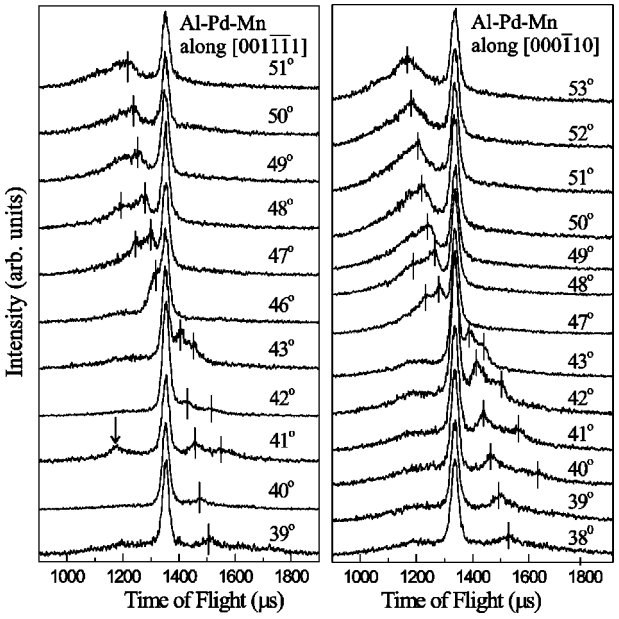

FIG. 9. Sets of TOF spectra from the fivefold *i*-Al-Pd-Mn (100000) surface along the [001$\bar{1}\bar{1}$1] and [000$\bar{1}$10] azimuths. Beam energy was 15 meV, sample temperature around 200 °C. The angles of incidence are shown above the spectra. The positions of single phonon peaks are marked by vertical lines. The peak indicated by an arrow is a decepton.

trast to the decagonal quasicrystals. The fivefold *i*-Al-Pd-Mn(100000) surface exhibits two high symmetry directions labeled by [001$\bar{1}\bar{1}$1] and [000$\bar{1}$10] (Ref. 29) as indicated in the LEED image in Fig. 7(a). Helium diffraction along these high symmetry directions reveals surface diffraction peaks at the surface projections of bulk reciprocal basis vectors [Figs. 7(b) and 7(c)]. The surface is clearly fivefold and not tenfold, as the intensities of peaks along [001111] are not symmetric with regard to a sign change of the wave vectors. This is apparent from the inner ring in the LEED image [Fig. 7(a)] and the peaks at ± 0.99 Å^{-1} and ± 1.6 Å^{-1} in He diffraction [Fig. 7(b)].

An illustration of the 2D reciprocal lattice based on the He diffraction spectra of Fig. 7 is given in Fig. 8. As the line scans along the two directions were measured under different experimental conditions, the specular intensities of two directions are slightly different and a normalization to the background intensity was chosen for the compilation of the 2D pattern.

For the determination of the surface phonon dispersion along the two high symmetry directions, sets of TOF spectra were recorded for beam energies between 13 and 22 meV. Selected spectra at 15 meV beam energy are presented in Fig. 9. As in the case of the tenfold surface of *d*-Al-Ni-Co, the TOF spectra consist of a central elastic peak, single phonon peaks, and background intensity. At small wave vectors the single phonon peaks are sharp and their linewidth is limited by the instrumental resolution, while at larger wave vectors their width cannot be determined accurately due to their decreasing intensity.

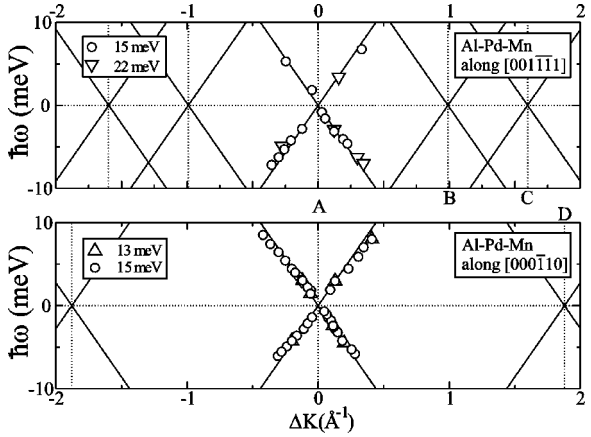

FIG. 10. The phonon dispersion relation of fivefold *i*-Al-Pd-Mn(100000) along the [001$\bar{1}\bar{1}$1] (top) and [000$\bar{1}$10] (bottom) azimuths. Different symbols represent the data obtained for different beam energies. The solid lines represent linear dispersion expected from the elastic moduli (Ref. 33) ($v_R = 3470$ m/s).

The dispersion relations derived from the TOF spectra are shown in Fig. 10. Again, the solid lines represent the linear dispersion with the Rayleigh mode velocity $v_R^{em} = 3470$ m/s derived from elastic moduli.[33]

Since *i*-Al-Pd-Mn is elastically isotropic,[32] it is fully characterized by two elastic constants or the two sound velocities $v_{L,T}$ of longitudinal and transversal (bulk) waves, respectively. The knowledge of the experimental sound velocities $v_L = (6300 \pm 300)$ m/s and $v_T = (3500 \pm 100)$ m/s measured by neutron scattering[9] is thus sufficient to derive an expected Rayleigh velocity v_R^{sv}. Following Ref. 31, we find $v_R^{sv} = (3250 \pm 100)$ m/s in agreement with our data (and consistent with v_R^{em} based on the elastic moduli).

In contrast to the *d*-Al-Ni-Co surface, the observation of phonon peaks is limited to the linear regime centered around the specular peak ($\Delta \mathbf{K} = 0$). We interpret this as due to the lower signal to noise ratio of the data and not due to a qualitative difference in the surface phonons of the tenfold Al-Ni-Co and fivefold Al-Pd-Mn surfaces.

IV. CONCLUSIONS

With the successful preparation of surfaces with high structural quality, it became possible to measure low-energy surface phonons on the tenfold surface of *d*-Al-Ni-Co and the fivefold surface of *i*-Al-Pd-Mn. Both surfaces show well-defined Rayleigh modes. Their Rayleigh sound velocities are isotropic and in good agreement with values derived from the elastic moduli of the respective bulk quasicrystals. As expected for surfaces with a moderate to low corrugation, the most intense phonon peaks are observed close to zero momentum transfer. For the tenfold surface of *d*-Al-Ni-Co, additional quasi-Brillouin-zone centers are identified at momentum transfers corresponding to strong Bragg peaks.

ACKNOWLEDGMENTS

Support from the DFG through the Schwerpunktprogramm ''Quasikristalle'' and under Grant No. Th732/1 is gratefully acknowledged.

*Corresponding author. Email address: wolfgang.theis@physik.fu-berlin.de

[1] D. Shechtman, I. Blech, D. Gratias, and J.W. Cahn, Phys. Rev. Lett. **53**, 1951 (1984).
[2] P.A. Thiel, A.I. Goldman, and C.J. Jenks, in *Physical Properties of Quasicrystals*, edited by Z.M. Stadnik (Springer, Berlin, 1999), and references therein.
[3] R. McGrath, J. Ledieu, E.J. Cox, and R.D. Diehl, J. Phys.: Condens. Matter **14**, R119 (2002), and references therein.
[4] J. Hafner and M. Krajčı, J. Phys.: Condens. Matter **5**, 2489 (1993).
[5] J. Hafner and M. Krajčı, Europhys. Lett. **21**, 31 (1993).
[6] M. Windisch, J. Hafner, M. Krajčıi, and M. Mihalkovic, Phys. Rev. B **49**, 8701 (1994).
[7] J. Hafner, M. Krajčı, and M. Mihalkovic, Phys. Rev. Lett. **76**, 2738 (1996).
[8] M. Quilichini and T. Janssen, Rev. Mod. Phys. **69**, 277 (1997).
[9] M. de Boissieu, M. Boudard, R. Bellissent, M. Quilichini, B. Hennion, R. Currat, A.I. Goldman, and C. Janot, J. Phys.: Condens. Matter **5**, 4945 (1993).
[10] M. de Boissieu, M. Boudard, H. Moudden, M. Quilichini, R. Bellissent, B. Hennion, R. Currat, A. Goldman, and C. Janot, J. Non-Cryst. Solids **153/154**, 552 (1993).
[11] M. Boudard, M. de Boissieu, S. Kycia, A.I. Goldman, B. Hennion, R. Bellissent, M. Quilichini, R. Currat, and C. Janot, J. Phys.: Condens. Matter **7**, 7299 (1995).
[12] A.I. Goldman, C. Stassis, R. Bellissent, H. Moudden, N. Pyka, and F.W. Gayle, Phys. Rev. B **43**, 8763 (1991).
[13] A.I. Goldman, C. Stassis, M. de Boissieu, R. Currat, C. Janot, R. Bellissent, H. Moudden, and F.W. Gayle, Phys. Rev. B **45**, 10 280 (1992).
[14] M. Quilichini, B. Hennion, G. Heger, S. Lefebvre, and A. Quivy, J. Phys. II **2**, 125 (1992).
[15] R.A. Brand, A.-J. Dianoux, and Y. Calvayrac, Phys. Rev. B **62**, 8849 (2000).
[16] F. Dugain, M. de Boissieu, K. Shibata, R. Currat, T.J. Sato, A.R. Kortan, J.-B. Suck, K. Hradil, F. Frey, and A.P. Tsai, Eur. Phys. J. B **7**, 513 (1999).
[17] M. Krisch, R.A. Brand, M. Chernikov, and H.R. Ott, Phys. Rev. B **65**, 134201 (2002).
[18] N.W. Ashcroft and N.D. Mermin, *Solid State Physics* (International Thomson Publishing, Philadelphia, 1976).
[19] K. Niizeki, J. Phys. A **22**, 4295 (1989).
[20] K. Niizeki and T. Akamatsu, J. Phys.: Condens. Matter **2**, 2759 (1990).
[21] L. Rayleigh, Proc. London Math. Soc. **17**, 4 (1887).
[22] M. Feuerbacher, C. Thomas, and K. Urban, in *Quasicrystals, Structure and Physical Properties*, edited by H.-R. Trebin (Wiley-VCH, Weinheim, 2003).
[23] P. Gille, R.-U. Barz, and L.M. Zhang, in *Quasicrystals, Structure and Physical Properties*, edited by H.-R. Trebin (Wiley-VCH, Weinheim, 2003).
[24] P. Gille, P. Dreier, M. Gräber, and T. Scholpp, J. Cryst. Growth **207**, 95 (1999).
[25] P. Ebert, F. Kluge, B. Grushko, and K. Urban, Phys. Rev. B **60**, 874 (1999).
[26] P. Ebert, M. Yurechko, F. Kluge, T. Cai, B. Grushko, P.A. Thiel, and K. Urban, Phys. Rev. B **67**, 024208 (2003).
[27] H.R. Sharma, Ph.D. thesis, Free University, Berlin, Germany 2002, http://www.diss.fu-berlin.de/2002/225
[28] J.P. Toennies, in *Surface Phonons*, Springer Series in Surface Sciences Vol. 21, edited by W. Kress and F.W. de Wette (Springer-Verlag, Berlin, 1991).
[29] W. Steurer and T. Haibach, in *Physical Properties of Quasicrystals*, edited by Z.M. Stadnik (Springer, Berlin, 1999).
[30] M.A. Chernikov, H.R. Ott, A. Bianchi, A. Migliori, and T.W. Darling, Phys. Rev. Lett. **80**, 321 (1998).
[31] A.A. Maradudin and G.I. Stegeman, in *Surface Phonons*, *Springer Series in Surface Sciences*, Vol. 21, edited by W. Kress and F.W. de Wette (Springer-Verlag, Berlin, 1991).
[32] P. Bak, Phys. Rev. B **32**, 5764 (1985).
[33] C.A. Swenson, I.R. Fisher, J.N.E. Anderson, and P.C. Canfield, Phys. Rev. B **65**, 184206 (2002).